Published in final edited form as:
Dev Dyn. 2012 March ; 241(3): 627–637. doi:10.1002/dvdy.23745.

Neogenin regulates Sonic hedgehog pathway activity during digit patterning

Mingi Hong, **Karen A. Schachter**[1], **Guoying Jiang**[1], and **Robert S. Krauss**[*]
Department of Developmental and Regenerative Biology, Mount Sinai School of Medicine, New York, NY 10029, USA

Abstract

Background—Digit patterning integrates signaling by the Sonic Hedgehog (SHH), FGF and BMP pathways. GLI3, a component of the SHH pathway, is a major regulator of digit number and identity. Neogenin (encoded by *Neo1*) is a cell surface protein that serves to transduce signals from several ligands, including BMPs, in various developmental contexts. Although neogenin is implicated in BMP signaling, it has not been linked to SHH signaling and its role in digit patterning is unknown.

Results—We report that *Neo1* mutant mice have preaxial polydactyly with low penetrance. Expression of SHH target genes, but not BMP target genes, is altered in *Neo1* mutant limb buds. Analysis of mice carrying mutations in both *Neo1* and *Gli3* reveals that although neogenin plays a role in constraint of digit numbers, suppressing polydactyly, it is also required for the severe polydactyly caused by loss of GLI3. Furthermore, embryo fibroblasts from *Neo1* mutant mice are sensitized to SHH pathway activation in vitro.

Conclusions—Our findings indicate that neogenin regulates SHH signaling in the limb bud to achieve proper digit patterning.

INTRODUCTION

Vertebrate limb bud development is a complex process that involves integration of multiple signaling pathways in spatiotemporal feedback networks (Tickle, 2006; Zeller et al., 2009). Sonic hedgehog (SHH) plays a critical role in patterning the anterior-posterior axis of the developing limb bud, specifying the number and identity of the digits (digit 1 being the most anterior and digit 5 the most posterior in the mouse) (Tickle, 2006; Zeller et al., 2009). SHH is produced by the zone of polarizing activity (ZPA), a group of mesenchymal cells at the posterior margin of the limb bud, and diffuses anteriorly in a graded fashion. Genetic and lineage analyses in the mouse and chick have led to models in which digit 1 forms independently of SHH, digit 2 and part of digit 3 are specified in a paracrine manner by low concentrations of SHH produced by the ZPA, and part of digit 3, and digits 4 and 5, are derived from descendants of ZPA cells themselves, dependent on autocrine SHH signaling (Harfe et al., 2004; Scherz et al., 2007). In addition to playing an early role in specifying digit identity, SHH is subsequently required for digit progenitor cells to proliferate into cartilage condensations (Towers et al., 2008; Zhu et al., 2008). Outgrowth of the limb bud in the proximal-distal axis is dependent on fibroblast growth factor (FGF) signaling by the apical ectodermal ridge (AER) at the distal tip of the limb bud (Tickle, 2006; Zeller et al.,

[*]Corresponding author: Robert S. Krauss, Department of Developmental and Regenerative Biology, Mount Sinai School of Medicine, New York, NY, 10029, USA. Phone: 212-241-2177; Fax: 212-860-9279; Robert.Krauss@mssm.edu.
[1]Present addresses:
K.S., Stem Cell Center, Department of Laboratory Medicine, Lund University, BMC B10, Lund 22184, Sweden
G.J., Genentech, Inc., 1 DNA Way, South San Francisco, California 94080, USA

2009). Positive feedback loops that integrate FGF signaling from the AER, SHH signaling from the ZPA, and bone morphogenetic protein (BMP) signaling in the mesenchyme and AER coordinate development of the limbs in multiple axes (Tickle, 2006; Zeller et al., 2009).

SHH activates signal transduction by binding its primary transmembrane receptor PTCH1, relieving inhibition of the signaling function of a second transmembrane protein, Smoothened (SMO) (for reviews, see Jiang and Hui, 2008; Varjosalo and Taipale, 2008). Signaling by SMO triggers a cascade that results in expression of target genes via the GLI family of transcription factors. In the absence of ligand, GLI3 (and to a lesser extent GLI2) undergoes proteolytic processing to produce a truncated protein that acts as a repressor of pathway target genes. SHH pathway signaling results in suppression of GLI proteolysis, and full-length GLI2 (and to a lesser extent GLI3) functions to activate pathway target genes. Among the targets are *Gli1* and *Ptch1* themselves. SHH signaling is also regulated by the cell surface proteins CDO, BOC and GAS1, which have overlapping function as co-receptors with PTCH1 and appear to sensitize cells in a developmental field to a given level of ligand (Kang et al., 2007; Allen et al., 2011; Bae et al., 2011; Izzi et al., 2011; Zhang et al., 2011).

Regulation of GLI3 processing is a critical aspect of SHH function in digit patterning. High levels of GLI3 repressor are present in the anterior region of the limb bud, which does not give rise to digits, and low levels are present in the posterior region, from which the digits develop (Tickle, 2006; Zeller et al., 2009). Mice lacking GLI3 are polydactylous, having 6–8 digits that lack clear identity, per limb. Furthermore, *Gli3;Shh* double mutants have the same digit phenotype as *Gli3* mutants, indicating that a major portion of SHH action in limb development is to inhibit formation of GLI3 repressor and that SHH itself is unnecessary for the polydactyly associated with loss of GLI3 (Litingtung et al., 2002; te Welscher et al., 2002).

Preaxial polydactyly (extra toes on the anterior side) is a frequent congenital abnormality in the human population, occurring in ~1 in 2000 births (Hill, 2007). Mutation of several different genes in the mouse results in preaxial polydactyly, and a common feature of these mutants is the formation of an ectopic, anterior SHH signaling center that results in expression of normally posterior-restricted genes and generation of the extra digit(s) (Hill, 2007). Among the genes whose mutation produces preaxial polydactyly are *Gli3* (*Extra-toes*), *Alx4* (*Strong's luxoid* [*lst*]) and *Bmp4* (Hui and Joyner, 1993; Dunn et al., 1997; Qu et al., 1997).

Neogenin is a cell surface transmembrane protein with four Ig domains and six fibronectin type III (FnIII) domains in its extracellular region and is involved in various physiological processes. Neogenin serves as a primary receptor for netrins and Repulsive Guidance Molecules (RGMs) to regulate axon guidance and other processes during CNS development (De Vries and Cooper, 2008). Neogenin also binds BMPs and RGMs to regulate BMP receptor signaling in endochondral bone development and iron metabolism (Lee et al., 2010; Zhou et al., 2010; Hagihara et al., 2011). Finally, netrin-neogenin signaling promotes skeletal myogenesis, where neogenin appears to work as part of a complex with the multifunctional co-receptor, CDO (itself an Ig/FnIII protein and a SHH co-receptor) (Kang et al., 2004; Bae et al., 2009). Neogenin therefore plays multiple developmental roles in a context-dependent manner. In this report we present another function of neogenin, in limb and digit patterning. A combination of genetic and gene expression analyses in the mouse and in vitro studies indicate that neogenin regulates limb and digit patterning through interactions with the SHH pathway.

RESULTS

Neo1$^{Gt/Gt}$ Mice Display Partially Penetrant Preaxial Polydactyly and Ectopic SHH Pathway Activity

Mice homozygous for a secretory gene-trap insertion in the *Neo1* gene (encoding neogenin; the *Neo1*^{Gt} allele) display perinatal lethality with ~20% survival by P21 (Bae et al., 2009). We noticed that some of the surviving animals had an extra preaxial digit, restricted to the right hindlimb. To obviate the complicating factor of perinatal lethality, we analyzed E17.5 or P0 embryos by staining skeletal preparations with Alizarin Red and Alcian Blue. Approximately 15% of *Neo1*$^{Gt/Gt}$ mice displayed either an extra digit 2 (as determined by the presence of three phalanges) anterior to digit 1 or a shift in identity of digit 1 to a digit 2-like phenotype, again based on the number of phalanges (Fig. 1A). Extra digits and identity shifts were seen only on the right hindlimb and were never seen in wild-type or *Neo1*$^{+/Gt}$ mice. Analysis of E13.5 embryos by whole mount in situ hybridization for expression of the early chondrogenesis marker *Sox9* revealed similar findings (Fig. 1B). Therefore, loss of neogenin results in right hindlimb preaxial polydactyly with low penetrance.

Digit progenitors are specified early in limb bud development (Zeller et al., 2009). *Neo1* is broadly expressed during development (Keeling et al., 1997; Bae et al., 2009). To assess *Neo1* expression in limb buds, we took advantage of the fact that the secretory gene-trap insertion leads to expression of *lacZ* from the *Neo1* locus. β-galactosidase activity was found throughout the mesenchyme in E10.5 and E11.5 hindlimb buds, but at much lower levels at the periphery of the limb bud, including the AER (Fig. 2A); a similar pattern was seen in forelimb buds (Bae et al., 2009). We also performed Western blot analyses on limb buds isolated from E11.5 wild-type or *Neo1*$^{Gt/Gt}$ mice. *Neo1*$^{Gt/Gt}$ limb buds had barely detectable neogenin protein, quantified as 2.2 – 6.8% the amount produced by wild-type limb buds (n=3; Figure 2B); wild-type and *Neo1*$^{Gt/Gt}$ mouse embryo fibroblasts (Bae et al., 2009) were used as controls (Figure 2B). This is consistent with the conclusion that the secretory gene-trap insertions are null or very strongly hypomorphic alleles (Mitchell et al., 2001).

Mice with preaxial polydactyly generally display an ectopic, anterior SHH signaling center in the limb bud. We therefore assessed whether this was present in *Neo1*$^{Gt/Gt}$ mice by whole mount in situ hybridization. The expression pattern of *Gli1* in E10.5 *Neo1*$^{+/+}$ and *Neo1*$^{Gt/Gt}$ limb buds was indistinguishable (data not shown). At E11.5, ectopic expression of the SHH target genes *Gli1* and *Ptch1* was detected at the anterior edge of the right hindlimb bud, but not other limb buds, in two of eight and two of ten (E11.5) *Neo1*$^{Gt/Gt}$ embryos, respectively, correlating with both the site and penetrance of polydactyly (Fig. 2C). Surprisingly, ectopic expression of *Shh* itself was not seen in E11.5 *Neo1*$^{Gt/Gt}$ embryos (n=8) (Fig. 2B). Our failure to detect an ectopic zone of *Shh* expression is unexpected, as this is generally seen in parallel with ectopic expression of *Gli1* and *Ptch1* in mouse models of preaxial polydactyly (Dunn et al., 1997; Qu et al., 1997). Given the relatively mild phenotype of *Neo1*$^{Gt/Gt}$ limbs, one possible explanation of this result may be that ectopic *Shh* occurred, but at a level sufficiently low to be difficult to detect with whole-mount in situ hybridization.

Bmp4$^{+/-}$ mice also show right hindlimb-specific, preaxial polydactyly with low penetrance (Dunn et al., 1997), and neogenin positively regulates BMP signaling during chondrogenesis of limb bones (Zhou et al., 2010). We therefore assessed expression of *Msx1* and *Msx2*, targets of BMP signaling, in the limb buds of *Neo1*$^{Gt/Gt}$ embryos. In contrast to SHH target genes, expression of *Msx1* and *Msx2* was not mispatterned or obviously diminished in these mutants (n=12 each) (Fig. 2C). Furthermore, no conspicuous change in *Bmp4* expression was observed in *Neo1*$^{Gt/Gt}$ limb buds (n=10) (Fig. 2C). Taken together, these findings

suggest that neogenin acts specifically to restrict SHH signaling in the limb bud and that its loss results in activation of this pathway in the anterior region.

Genetic Interaction Between *Neo1* and *Gli3*

A major aspect of SHH function in limb and digit patterning is to block formation of GLI3 repressor in the posterior limb bud. The limbs of mice lacking GLI3 have 6–8 digits of indeterminate identity, and *Gli3* is epistatic to *Shh* (Litingtung et al., 2002; te Welscher et al., 2002). Mice heterozygous for *Gli3* display prexial polysyndactyly, and *Gli3* interacts genetically with other genes that produce similar phenotypes (Dunn et al., 1997; Panman et al., 2005). We therefore assessed the effect of removing one or both copies of *Gli3* from $Neo1^{Gt/Gt}$ mice. On this background, we found that $Gli3^{+/Xt\text{-}J}$ mice had preaxial polysyndactyly of the forelimbs with high penetrance and of the hindlimbs with lower penetrance; twice as many right limbs were affected as left limbs, for both forelimbs and hindlimbs (Table 1, Fig. 3). $Gli3^{+/Xt\text{-}J};Neo1^{Gt/Gt}$ mice showed a strikingly altered phenotype from $Gli3^{+/Xt\text{-}J}$ mice. Loss of neogenin increased the percentage of $Gli3^{+/Xt\text{-}J}$ hindlimbs with preaxial digits by ~3.5-fold (right hindlimbs) and ~4.9-fold (left hindlimbs) (Table 1, Fig. 3A). Loss of both copies of *Neo1* was required for this effect, as $Gli3^{+/Xt\text{-}J};Neo1^{+/Gt}$ mice were similar to $Gli3^{+/Xt\text{-}J};Neo1^{+/+}$ mice (Table 1). Consistent with this enhancement of polydactyly, five of seven $Gli3^{+/Xt\text{-}J};Neo1^{Gt/Gt}$ mice displayed ectopic *Ptch1* expression in the anterior region of their hindlimb buds (Fig. 4). As with $Neo1^{Gt/Gt}$ mice, however, we were unable to detect ectopic anterior *Shh* expression itself in $Gli3^{+/Xt\text{-}J};Neo1^{Gt/Gt}$ limb buds (Fig. 4).

In contrast to the observation that loss of neogenin enhanced hindlimb polydactyly in $Gli3^{+/Xt\text{-}J}$ mice, we found that 22 of 23 $Gli3^{+/Xt\text{-}J};Neo1^{Gt/Gt}$ mice had five digits on both their forelimbs (Table 1, Fig. 3A). Therefore, although removal of *Neo1* strongly enhanced the hindlimb polydactyly seen in $Gli3^{+/Xt\text{-}J}$ mice, it almost completely suppressed the forelimb polydactyly of these animals.

The tendency toward suppression of polydactyly in *Gli3* mutants by loss of neogenin was even more pronounced in $Gli3^{Xt\text{-}J/Xt\text{-}J};Neo1^{Gt/Gt}$ mice. The average number of digits per limb in these double homozygous mutants was 5.7, reduced from 6.6 in $Gli3^{Xt\text{-}J/Xt\text{-}J};Neo1^{+/+}$ animals (Table 2 and Fig. 3A). Furthermore, while no $Gli3^{Xt\text{-}J/Xt\text{-}J};Neo1^{+/+}$ mice had five digits on any limbs, 75% of $Gli3^{Xt\text{-}J/Xt\text{-}J};Neo1^{Gt/Gt}$ mice had five digits on at least one limb, and, overall, >40% of limbs from the double homozygous mutant mice had only five digits (Table 2). Finally, when scoring limbs with seven or more digits, a dosage-sensitive role for *Neo1* was observed, in that 50% of the limbs of $Gli3^{Xt\text{-}J/Xt\text{-}J};Neo1^{+/+}$ mice had at least seven digits, whereas 21.4% of $Gli3^{Xt\text{-}J/Xt\text{-}J};Neo1^{+/Gt}$ mice and 12.5% of $Gli3^{Xt\text{-}J/Xt\text{-}J};Neo1^{Gt/Gt}$ mice did (Table 2). Therefore, neogenin is required for polydactyly associated with loss of *Gli3*. The indeterminate digit identity seen in $Gli3^{Xt\text{-}J/Xt\text{-}J}$ mice, however, was not rescued by further loss of neogenin, even in limbs with five digits. $Gli3^{Xt\text{-}J/Xt\text{-}J};Neo1^{+/+}$ animals displayed ectopic anterior expression of *Shh* and *Ptch1* (Fig. 4). Despite the suppression of polydactyly by genetic removal of neogenin, all $Gli3^{Xt\text{-}J/Xt\text{-}J};Neo1^{Gt/Gt}$ mice (n=4) showed ectopic anterior expression of *Shh* and *Ptch1* (Fig. 4).

A genetic interaction between *Gli3* and *Neo1* was also observed in development of the zeugopod (radius and ulna in the forelimb; tibia and fibula in the hindlimb). $Gli3^{Xt\text{-}J/Xt\text{-}J};Neo1^{+/+}$ mice showed normal formation of the radius and had a rudimentary tibia (Fig. 3B). In contrast, 69% (11 of 16) of $Gli3^{Xt\text{-}J/Xt\text{-}J};Neo1^{Gt/Gt}$ double mutants lacked both a radius and a tibia. The ulna and fibula formed normally in these mice. No defects in zeugopod patterning were seen in mice lacking only neogenin (data not shown). The suppression of polydactyly and loss of the radius in $Gli3^{Xt\text{-}J/Xt\text{-}J};Neo1^{Gt/Gt}$ mice is very similar to the phenotype of mice mutant for both *Gli3* and *Alx4* (Panman et al., 2005). We

therefore examined expression of *Alx4* in the limb buds of E11.5 $Neo1^{Gt/Gt}$ embryos. *Alx4* expression was restricted to the proximal anterior region in wild-type mice, and this pattern of expression was not obviously changed in $Neo1^{Gt/Gt}$ mice (Fig. 2). Therefore, defects in limb patterning that occur upon loss of neogenin are unlikely to arise by a simple loss of *Alx4* expression.

$Neo1^{Gt/Gt}$ MEFs Are Sensitized to Activation of the SHH Pathway but Neogenin Does Not Bind SHH

To test further the hypothesis that neogenin is a negative regulator of the SHH signaling pathway, we analyzed primary MEFs from $Neo1^{+/+}$ and $Neo1^{Gt/Gt}$ embryos. Multiple isolates of such cells were treated with either recombinant N-terminal fragment of SHH (SHH-N) or the SMO agonist SAG, and induction of endogenous *Gli1* and *Ptch1* was quantified by qRT-PCR. *Gli1* expression in control $Neo^{+/+}$ cells was increased 10-fold by both SHH-N and SAG; consistent with the *in vivo* results, the amount of *Gli1* induced in $Neo^{Gt/Gt}$ cells was more than twice that seen in the $Neo^{+/+}$ cells, with either agonist (Fig. 5A). Somewhat surprisingly, there was not a significant difference between $Neo1^{+/+}$ and $Neo1^{Gt/Gt}$ MEFs in SHH-N- or SAG-dependent expression of *Ptch1*, which was induced less robustly in these cells than *Gli1* (Fig. 5A). Neogenin's effects on SHH pathway target gene expression may therefore differ somewhat at distinct loci and in vivo vs. in vitro.

The neogenin ectodomain contains Ig and FnIII repeats, similar to the SHH co-receptors CDO and BOC (Kang et al., 1997; Kang et al., 2002). Furthermore, neogenin forms cis complexes with CDO and BOC (Kang et al., 2004). We therefore tested whether neogenin binds SHH in vitro. Recombinant, secreted proteins comprising the ectodomains of neogenin or, as a positive control, CDO, fused in-frame with the Fc region of human IgG were bound to protein-A sepharose. A soluble SHH-N::AP fusion protein (consisting of the N-terminal portion of SHH with alkaline phosphatase (AP) fused to its carboxy terminus) or, as a control, AP itself, were then allowed to bind the neogenin-Fc and CDO-Fc matrices. Under conditions where SHH-N::AP bound specifically to CDO, no binding of SHH-N::AP to neogenin was observed (Fig. 5B). Therefore, neogenin is a negative regulator of SHH signaling in vivo and in vitro, but its effects are unlikely to occur through direct interaction with SHH ligand.

DISCUSSION

Limb and digit patterning are governed by interactions between the SHH, BMP and FGF pathways (Tickle, 2006; Zeller et al., 2009). Mutations in specific components or regulators of these pathways result in patterning defects, such as polydactyly. In this report we identify a role for *Neo1* in limb and digit patterning and as a genetic modifier of *Gli3*, which encodes a component of the SHH pathway and is a critical regulator of digit number and identity.

Neogenin is a multifunctional cell surface receptor. It has a large ectodomain, single transmembrane region and long cytoplasmic tail. It serves as a primary receptor for netrins and RGMs in CNS development, and binding of these ligands to the neogenin ectodomain results in association of the cytoplasmic tail with signaling proteins and consequent signal transduction (De Vries and Cooper, 2008). RGMs also act as BMP co-receptors, and both neogenin and RGMs bind directly to BMPs (Corradini et al., 2009; Hagihara et al., 2011). Moreover, neogenin promotes BMP signaling during limb bone chondrogenesis (Zhou et al., 2010). We find that ~15% of mice homozygous for a gene-trap mutation in *Neo1* display preaxial polydactyly of the right hindlimb. $Bmp4^{+/-}$ mice have a very similar phenotype, including both the right hindlimb specificity and low penetrance (Dunn et al., 1997). One logical possibility, therefore, is that neogenin promotes signaling through BMPs, and that $Bmp4^{+/-}$ and $Neo1^{Gt/Gt}$ mice have equivalent signaling defects, resulting in nearly identical

digit patterning phenotypes. However, *Neo1*$^{Gt/Gt}$ mice did not show obvious alterations in expression of two BMP targets, *Msx1* and *Msx2*, or of *Bmp4* itself, during limb bud development. Furthermore, the genetic interactions of *Gli3* with *Bmp4* vs. *Neo1* were distinct. Dunn et al. reported that removal of one copy of *Bmp4* from *Gli3*$^{+/Xt\text{-}J}$ mice enhanced both forelimb and hindlimb polydactyly (Dunn et al., 1997), whereas removal of both copies of *Neo1* from *Gli3*$^{+/Xt\text{-}J}$ mice enhanced hindlimb polydactyly but strongly suppressed forelimb polydactyly. Taken together, these results are inconsistent with the notion that neogenin exerts its effects on digit patterning simply by promoting BMP activity.

The reason for the right hindlimb specificity of the polydactyly in *Neo1*$^{Gt/Gt}$ mice is unclear. Preference for right over left limbs (in both forelimbs and hindlimbs) has been observed with various digit patterning defects induced by mutations or teratogens (Layton and Hallesay, 1965; Dunn et al., 1997; Eggenschwiler et al., 1997; Zákány et al., 2004), but mechanistic insight into this phenomenon is lacking. One possibility is that there are subtle differences in signal timing or strength between right and left limbs that render the right limbs more sensitive to perturbation than the left limbs, but this is speculative, and we have not observed reproducible right-left differences in the expression of the genes analyzed in this study.

Analysis of *Gli3;Neo1* double mutants revealed that *Neo1* is a complex modifier of *Gli3* function in development of both the autopod and zeugopod. The facts that homozygous mutation of *Neo1* alone resulted in preaxial polydactyly and enhanced hindlimb preaxial polydactyly in *Gli3*$^{+/Xt\text{-}J}$ mice, indicates that neogenin functions to limit digit number. However, forelimb preaxial polydactyly was suppressed in *Gli3*$^{+/Xt\text{-}J}$*;Neo1*$^{Gt/Gt}$ mice; furthermore, double homozygous (*Gli3*$^{Xt\text{-}J/Xt\text{-}J}$*;Neo1*$^{Gt/Gt}$) mutants showed strong suppression of the extreme polydactyly seen in *Gli3*$^{Xt\text{-}J/Xt\text{-}J}$ mice on all limbs. Therefore, neogenin is also required for polydactyly associated with lack of *Gli3*. Additionally, *Gli3*$^{Xt\text{-}J/Xt\text{-}J}$*;Neo1*$^{Gt/Gt}$ mice lacked a radius and a tibia (the anterior elements of the zeugopod), whereas *Gli3*$^{Xt\text{-}J/Xt\text{-}J}$ mice had a normal radius and rudimentary tibia. These findings are strikingly similar to what is observed with *Alx4*. *Alx4*$^{-/-}$ mice have preaxial polydactyly (more strongly than do *Neo1*$^{Gt/Gt}$ mice), but *Gli3*$^{Xt\text{-}J/Xt\text{-}J}$*;Alx4*$^{-/-}$ double homozygous mutants display suppression of polydactyly and loss of anterior zeugopod elements (Panman et al., 2005). *Alx4* is expressed in the anterior aspect of the limb bud (Qu et al., 1997) but its expression was not conspicuously altered in *Neo1*$^{Gt/Gt}$ mice. As *Neo1* is expressed throughout the limb bud mesenchyme, a connection to *Alx4* is not immediately apparent. Why removal of *Neo1* (or *Alx4*) from *Gli3*$^{Xt\text{-}J/Xt\text{-}J}$ mice results in these phenotypes is not clear. One possibility is that they arise from abnormally enhanced SHH signaling above and beyond what occurs in the absence of any GLI3 repressor. Although loss of GLI3 repressor might be viewed as maximally deregulating pathway activity in the context of limb bud patterning, we are not aware of previous studies in which positive SHH signaling is deliberately further upregulated in the limb bud in the absence of GLI3 (e.g., in conditional *Gli3*$^{-/-}$*;Ptch1*$^{-/-}$ or *Gli3*$^{-/-}$*;Sufu*$^{-/-}$ mice).

Consistent with the notion that neogenin negatively regulates SHH pathway activity in the limb bud, *Neo1*$^{Gt/Gt}$ mice had ectopic anterior expression of the SHH targets *Gli1* and *Ptch1* on the right hindlimb at frequencies similar to those at which they showed preaxial polydactyly. Such ectopic SHH signaling centers are typically observed in mice with preaxial polydactyly, including *Bmp4*$^{+/-}$ mice (Dunn et al., 1997; Hill, 2007). However, primary MEFs isolated from *Neo1*$^{Gt/Gt}$ embryos were also sensitized to SHH pathway signaling in vitro, suggesting a more direct role for neogenin in SHH signaling. *Neo1*$^{Gt/Gt}$ MEFs induced *Gli1* expression to a significantly greater extent than *Neo1*$^{+/+}$ MEFs when treated with recombinant SHH ligand or with the SMO agonist, SAG. Loss of neogenin in MEFs was not, however, sufficient to activate SHH pathway activity in the absence of SHH

ligand or SAG. Taken together, these results suggest that neogenin functions as a negative regulator of ligand-initiated SHH pathway signaling in the limb bud. The fact that *Neo1*$^{Gt/Gt}$ MEFs were sensitized to both SHH and SAG, argues that neogenin exerts its effects at the level of SMO or downstream of SMO. Neogenin binds to CDO and BOC, which are SHH co-receptors. One intriguing idea is that when neogenin associates with CDO and BOC it prevents or diminishes their participation in SHH signal reception. However, if this were so it would be expected that *Neo1*$^{Gt/Gt}$ MEFs would be sensitized to SHH, but not to activation of the pathway at the level of SMO (i.e., by SAG), yet these cells were sensitized to SAG, too. We have previously found that, in addition to binding SHH, CDO and BOC can also influence SHH pathway signaling in vitro at a downstream point, at the level of GLI factors (Zhang et al., 2006), but the mechanism is unclear, and where and when such an activity may occur in vivo is not known. It should also be mentioned that the polydactyly seen in *Gli3*$^{Xt\text{-}J/Xt\text{-}J}$ mice is independent of *Shh* (Litingtung et al., 2002; te Welscher et al., 2002), and it is not proven that the polydactyly caused by loss of neogenin requires ectopic *Shh* expression. Furthermore, the effects of neogenin on SHH signaling may be less direct than the mechanisms proposed above.

The genes that encode several of the components of the SHH pathway are transcriptional targets of the pathway also, including *Ptch1*, *Hhip1*, *Gli1*, *Cdo*, *Boc* and *Gas1*, resulting in a complex feedback network (Kang et al., 2007; Dessaud et al., 2008). It was recently reported that *Neo1* is a direct target of SHH/GLI signaling in cultured cells and during zebrafish development (Milla et al., 2012). Therefore, *Neo1* may belong to this group of factors that are both regulators and targets of the Hedgehog pathway and may be a component of the feedback network.

In conclusion, our results demonstrate that the multifunctional receptor neogenin is a regulator of limb and digit patterning, likely as a modifier of SHH and GLI3 function. These findings, combined with other studies on the roles of neogenin in netrin, RGM and BMP signaling reveal that this receptor is exceptionally versatile in its actions during development.

EXPERIMENTAL PROCEDURES

Mice

Mice carrying a secretory gene-trap vector insertion into intron 7 of the *Neo1* gene (the *Neo1*$^{Gt(KST265)Byg}$ allele, abbreviated *Neo1*^{Gt}) and on a largely C57BL/6 background were previously described (Leighton et al., 2001; Mitchell et al., 2001; Bae et al., 2009). C57BL/6J.*Gli3*$^{Xt\text{-}J}$ mice, carrying a spontaneous deletion in the *Gli3* locus (Hui and Joyner, 1993) were obtained from the Jackson Laboratory. Noon of the plug date was designated E0.5. All experiments were performed according to an Institutional Animal Care and Use Committee-approved protocol.

In situ hybridization, β-galactosidase staining and skeletal staining

For whole-mount RNA in situ hybridization, embryos were prepared essentially as described previously (Mulieri et al., 2002), except that they were treated with 10 μg/ml proteinase K (QIAGEN) in phosphate-buffered saline, 0.1% Tween-20 (PBT) according to stage (E10.5, 10 min; E11.5, 15 min). Embryos were rinsed, postfixed, and hybridized with digoxygenin-labeled probe in hybridization mix [50% formamide, 1.3× SSC, 5 mM EDTA, 50 μg /ml yeast RNA, 0.2% Tween 20, 0.5% 3-[(3-cholamidopropyl) dimethylammonio] propanesulfonate, and 100 μg /ml heparin] overnight at 65°C. After washing and blocking, embryos were incubated overnight with alkaline phosphatase-conjugated anti-digoxigenin antibody (1:2000; Roche) in blocking buffer (2% blocking reagent [Roche]), 20% heat-

inactivated lamb serum in 100 mM maleic acid, pH 7.5, 150 mM NaCl, and 0.1% Tween-20 [MABT]). After washing in Tris-buffered saline with 0.1% Tween-20 (TBST) and 100 mm NaCl, 100 mm Tris-HCl, pH 9.5, 50 mm $MgCl_2$, and 0.1% Tween-20 (NTMT), signals were developed using BM Purple AP Substrate (Roche).

Dissected embryos were stained for β-galactosidase activity essentially as described previously (Nait-Oumesmar et al., 2002) with the exception that fixation time was dependent on the age of the embryo. All steps except incubation with staining solution were performed at room temperature. Embryos were permeabilized for 2 hours in phosphate-buffered saline (PBS), pH 7.0, 2 mM MgCl2, 0.01% NP-40, and 0.02% sodium deoxycholate. Staining solution was identical to the above permeabilization buffer, supplemented with 17.5 mM each $K_3Fe(CN)_6$ and $K_4Fe(CN)_6$ and 1 mg/ml 5-bromo-4-chloro-3-indolyl-β-d-galactoside (Roche). Whole mount embryos were dehydrated into 80% glycerol and PBS for photography.

Bones and cartilage of late stage embryos were stained with Alizarin red and Alcian blue as described (Tribioli and Lufkin, 1999). Briefly, E18.5 embryos were eviscerated, fixed in 95% ethanol for 4–5 days and transferred to acetone for 3 days. Embryos were then rinsed with water and stained for 24 hours in 0.05% Alcian Blue in 20% glacial acetic acid and an 80% dilution of 95% ethanol. After washing in 95% ethanol for 2–3 days, soft tissues were dissolved in 1% KOH for 1 hour and stained in 0.75% Alizarin Red in 1% KOH for 4 hours. Stained embryos were kept in 20% glycerol/1% KOH until skeletons became clearly visible. Embryos were transferred into 50% glycerol, 80% glycerol and 100% glycerol for photography and storage.

Western blot analysis

Limb buds were dissected from E11.5 embryos and all four from each embryo were pooled together to prepare extracts, as previously described (Bae et al., 2009). One mg of limb bud extracts and 100 mg of mouse embryo fibroblast extracts were separated on a 7% SDS-PAGE gel and transferred to a PVDF membrane and probed with antibodies to neogenin (Santa Cruz) and pan-cadherin (Sigma). The signals were quantified by ImageJ.

SHH signaling in vitro

Primary mouse embryo fibroblasts (MEFs) were generated from *Neo1*$^{+/+}$ and *Neo1*$^{Gt/Gt}$ embryos at E14.5 by standard protocols (Sun and Taneja, 2007) and cultured in Dulbecco modified Eagle medium (DMEM) containing 10% fetal bovine serum. MEFs were treated with 300 ng/ml of ShhN or 300 nM Smoothened agonist (SAG; EMD Chemicals) for 24 hours. Total RNA was extracted using Trizol (Invitrogen) according to the manufacture's protocol. cDNA was synthesized from total RNA using SuperScript III First Strand Synthesis System (Invitrogen). Quantitative real-time PCR analysis of *Gli1 and Ptch1* expression was performed using PerfeCta SYBR Green FastMix for iQ (Quanta Biosciences) with a BioRad iCycler iQ5. Data were normalized to *Gapdh* expression and presented as fold-change over PBS-treated controls. qPCR promers for *Gapdh*, *Gli1* and *Ptch1* were from the Harvard PrimerBank. (PrimerBank Ids: 6679937a1, 6754002a1 and 6679519a1, respectively). Two independent isolates of *Neo1*$^{+/+}$ MEFs and three independent isolates of *Neo1*$^{Gt/Gt}$ MEFs were analyzed in duplicate in three separate experiments.

In vitro binding assays

Recombinant, secreted proteins comprising the ectodomains of neogenin or Cdo, fused in-frame with the Fc region of human IgG (Ng-Fc and Cdo-Fc, respectively) were produced in 293T cells and bound to protein-A sepharose. Shh::AP or, as a control, AP itself, were

produced similarly and allowed to bind the Ng-Fc and Cdo-Fc matrices, which were then washed exhaustively. Bound AP activity was quantified with AP yellow liquid substrate.

Acknowledgments

We thank J. Helms, B. Harfe, B. Allen, A, McMahon and X. Sun for riboprobe vectors. This work was supported by grants from the NIH and T.J. Martell Foundation to RSK.

REFERENCES

Allen BL, Song JY, Izzi L, Althaus IW, Kang J-S, Charron F, RS Krauss RS, McMahon AP. Overlapping roles and collective requirement for the co-receptors Gas1, Cdo and Boc in Shh pathway function. Dev Cell. 2011; 20:775–787. [PubMed: 21664576]

Bae GU, Domené S, Roessler E, Schachter K, Kang JS, Muenke M, Krauss RS. Mutations in CDON, Encoding a Hedgehog Receptor, Result in Holoprosencephaly and Defective Interactions with Other Hedgehog Receptors. Am J Hum Genet. 2011; 89:231–240. [PubMed: 21802063]

Bae GU, Yang YJ, Jiang G, Hong M, Lee HJ, Tessier-Lavigne M, Kang JS, Krauss RS. Neogenin regulates skeletal myofiber size and focal adhesion kinase and extracellular signal-regulated kinase activities in vivo and in vitro. Mol Biol Cell. 2009; 20:4920–4931. [PubMed: 19812254]

Corradini E, Babitt JL, Lin HY. The RGM/DRAGON family of BMP co-receptors. Cytokine Growth Factor Rev. 2009; 20:389–398. [PubMed: 19897400]

De Vries M, Cooper HM. Emerging roles for neogenin and its ligands in CNS development. J Neurochem. 2008; 106:1483–1492. [PubMed: 18485097]

Dessaud E, McMahon AP, Briscoe J. Pattern formation in the vertebrate neural tube: a sonic hedgehog morphogen-regulated transcriptional network. Development. 2008; 135:2489–2503. [PubMed: 18621990]

Dunn NR, Winnier GE, Hargett LK, Schrick JJ, Fogo AB, Hogan BL. Haploinsufficient phenotypes in Bmp4 heterozygous null mice and modification by mutations in Gli3 and Alx4. Dev Biol. 1997; 188:235–247. [PubMed: 9268572]

Eggenschwiler J, Ludwig T, Fisher P, Leighton PA, Tilghman SM, Efstratiadis A. Mouse mutant embryos overexpressing IGF-II exhibit phenotypic features of the Beckwith- Wiedemann and Simpson-Golabi-Behmel syndromes. Genes Dev. 1997; 11:3128–3142. [PubMed: 9389646]

Hagihara M, Endo M, Hata K, Higuchi C, Takaoka K, Yoshikawa H, Yamashita T. Neogenin, a receptor for bone morphogenetic proteins. J Biol Chem. 2011; 286:5157–5165. [PubMed: 21149453]

Harfe BD, Scherz PJ, Nissim S, Tian H, McMahon AP, Tabin CJ. Evidence for an expansion-based temporal Shh gradient in specifying vertebrate digit identities. Cell. 2004; 118:517–528. [PubMed: 15315763]

Hill RE. How to make a zone of polarizing activity: insights into limb development via the abnormality preaxial polydactyly. Dev Growth Differ. 2007; 49:439–448. [PubMed: 17661738]

Hui CC, Joyner AL. A mouse model of greig cephalopolysyndactyly syndrome: the extratoesJ mutation contains an intragenic deletion of the Gli3 gene. Nat Genet. 1993; 3:241–246. [PubMed: 8387379]

Izzi L, Lévesque M, Morin S, Laniel D, Wilkes BC, Mille F, Krauss RS, McMahon AP, Allen BL, Charron F. Boc and Gas1 each form distinct Shh receptor complexes with Ptch1 and are required for Shh-mediated cell proliferation. Dev Cell. 2011; 20:788–801. [PubMed: 21664577]

Jiang J, Hui CC. Hedgehog signaling in development and cancer. Dev Cell. 2008; 15:801–812. [PubMed: 19081070]

Kang J-S, Gao M, Feinleib JL, Cotter PD, Guadagno SN, Krauss RS. CDO: an oncogene-, serum-, and anchorage-regulated member of the Ig/fibronectin type III repeat family. J. Cell Biol. 1997; 138:203–213. [PubMed: 9214393]

Kang J-S, Mulieri PJ, Hu Y, Taliana L, Krauss RS. BOC, an Ig superfamily member, associates with CDO to positively regulate myogenic differentiation. EMBO J. 2002; 21:114–124. [PubMed: 11782431]

Kang J-S, Yi M-J, Zhang W, Feinleib JL, Cole F, Krauss RS. Netrins and neogenin promote myotube formation. J Cell Biol. 2004; 167:493–504. [PubMed: 15520228]

Kang JS, Zhang W, Krauss RS. Hedgehog signaling: cooking with Gas1. Sci STKE. 2007; 403:pe50. [PubMed: 17848687]

Keeling SL, Gad JM, Cooper HM. Mouse Neogenin, a DCC-like molecule, has four splice variants and is expressed widely in the adult mouse and during embryogenesis. Oncogene. 1997; 15:691–700. [PubMed: 9264410]

Layton WMJ, Hallesay DW. Deformity of forelimb in rats: association with high doses of acetazolamide. Science. 1965; 149:306–308. [PubMed: 14300527]

Lee DH, Zhou LJ, Zhou Z, Xie JX, Jung JU, Liu Y, Xi CX, Mei L, Xiong WC. Neogenin inhibits HJV secretion and regulates BMP-induced hepcidin expression and iron homeostasis. Blood. 2010; 115:3136–3145. [PubMed: 20065295]

Leighton PA, Mitchell KJ, Goodrich LV, Lu X, Pinson K, Scherz P, Skarnes WC, Tessier-Lavigne M. Defining brain wiring patterns and mechanisms through gene trapping in mice. Nature. 2001; 410:174–179. [PubMed: 11242070]

Litingtung Y, Dahn RD, Li Y, Fallon JF, Chiang C. Shh and Gli3 are dispensable for limb skeleton formation but regulate digit number and identity. Nature. 2002; 418:979–983. [PubMed: 12198547]

Milla LA, Cortes CR, Hodar CQ, Onate MG, Cambiazo V, Burgess SM, Palma V. Yeastbased assay identifies novel Shh/Gli target genes in vertebrate development. BMC Genomics. 2012; 13:2. [PubMed: 22214306]

Mitchell KJ, Pinson KI, Kelly OG, Brennan J, Zupicich J, Scherz P, Leighton PA, Goodrich LV, Lu X, Avery BJ, Tate P, Dill K, Pangilinan E, Wakenight P, Tessier-Lavigne M, Skarnes WC. Functional analysis of secreted and transmembrane proteins critical to mouse development. Nat. Genet. 2001; 28:241–249. [PubMed: 11431694]

Mulieri PM, Kang J-S, Sassoon DA, Krauss RS. Expression of the *boc* gene during murine embryogenesis. Dev. Dyn. 2002; 223:379–388. [PubMed: 11891987]

Nait-Oumesmar B, Stecca B, Fatterpekar G, Naidich T, Corbin J, Lazzarini RA. Ectopic expression of *Gcm1* induces congenital spinal cord abnormalities. Development. 2002; 129:3957–3964. [PubMed: 12135932]

Panman L, Drenth T, Tewelscher P, Zuniga A, Zeller R. Genetic interaction of Gli3 and Alx4 during limb development. Int J Dev Biol. 2005; 49:443–448. [PubMed: 15968591]

Qu S, Niswender KD, Ji Q, van der Meer R, Keeney D, Magnuson MA, Wisdom R. Polydactyly and ectopic ZPA formation in Alx-4 mutant mice. Development. 1997; 124:3999–4008. [PubMed: 9374397]

Scherz PJ, McGlinn E, Nissim S, Tabin CJ. Extended exposure to Sonic hedgehog is required for patterning the posterior digits of the vertebrate limb. Dev Biol. 2007; 308:343–354. [PubMed: 17610861]

Sun H, Taneja R. Analysis of transformation and tumorigenicity using mouse embryonic fibroblast cells. Methods Mol Biol. 2007; 383:303–310. [PubMed: 18217693]

te Welscher P, Zuniga A, Kuijper S, Drenth T, Goedemans HJ, Meijlink F, Zeller R. Progression of vertebrate limb development through SHH-mediated counteraction of GLI3. Science. 2002; 298:827–830. [PubMed: 12215652]

Tickle C. Making digit patterns in the vertebrate limb. Nat Rev Mol Cell Biol. 2006; 7:45–53. [PubMed: 16493412]

Towers M, Mahood R, Yin Y, Tickle C. Integration of growth and specification in chick wing digit-patterning. Nature. 2008; 452:882–886. [PubMed: 18354396]

Tribioli C, Lufkin T. The murine *Bapx1* homeobox gene plays a critical role in embryonic development of the axial skeleton and spleen. Development. 1999; 126:5699–5711. [PubMed: 10572046]

Varjosalo M, Taipale J. Hedgehog: functions and mechanisms. Genes Dev. 2008; 22:2454–2472. [PubMed: 18794343]

Zákány J, Kmita M, Duboule D. A dual role for Hox genes in limb anterior-posterior asymmetry. Science. 2004; 304:1669–1672. [PubMed: 15192229]

Zeller R, López-Ríos J, Zuniga A. Vertebrate limb bud development: moving towards integrative analysis of organogenesis. Nat Rev Genet. 2009; 10:845–858. [PubMed: 19920852]

Zhang W, Hong M, Bae G-U, Kang J-S, Krauss RS. *Boc* modifies the holoprosencephaly spectrum of *Cdo* mutant mice. Dis Model Mech. 2011; 4:368–380. [PubMed: 21183473]

Zhang W, Kang J-S, Cole F, Yi MJ, Krauss RS. Cdo functions at multiple points in the Sonic Hedgehog pathway, and Cdo-deficient mice accurately model human holoprosencephaly. Dev Cell. 2006; 10:657–665. [PubMed: 16647303]

Zhou Z, Xie J, Lee D, Liu Y, Jung J, Zhou L, Xiong S, Mei L, Xiong WC. Neogenin regulation of BMP-induced canonical Smad signaling and endochondral bone formation. Dev Cell. 2010; 19:90–102. [PubMed: 20643353]

Zhu J, Nakamura E, Nguyen MT, Bao X, Akiyama H, Mackem S. Uncoupling Sonic hedgehog control of pattern and expansion of the developing limb bud. Dev Cell. 2008; 14:624–632. [PubMed: 18410737]

Bullet points

- *Neo1* mutant mice have preaxial polydactyly with low penetrance
- *Neo1* interacts genetically with *Gli3* in a complex manner
- Neogenin regulates SHH signaling in vivo and in vitro

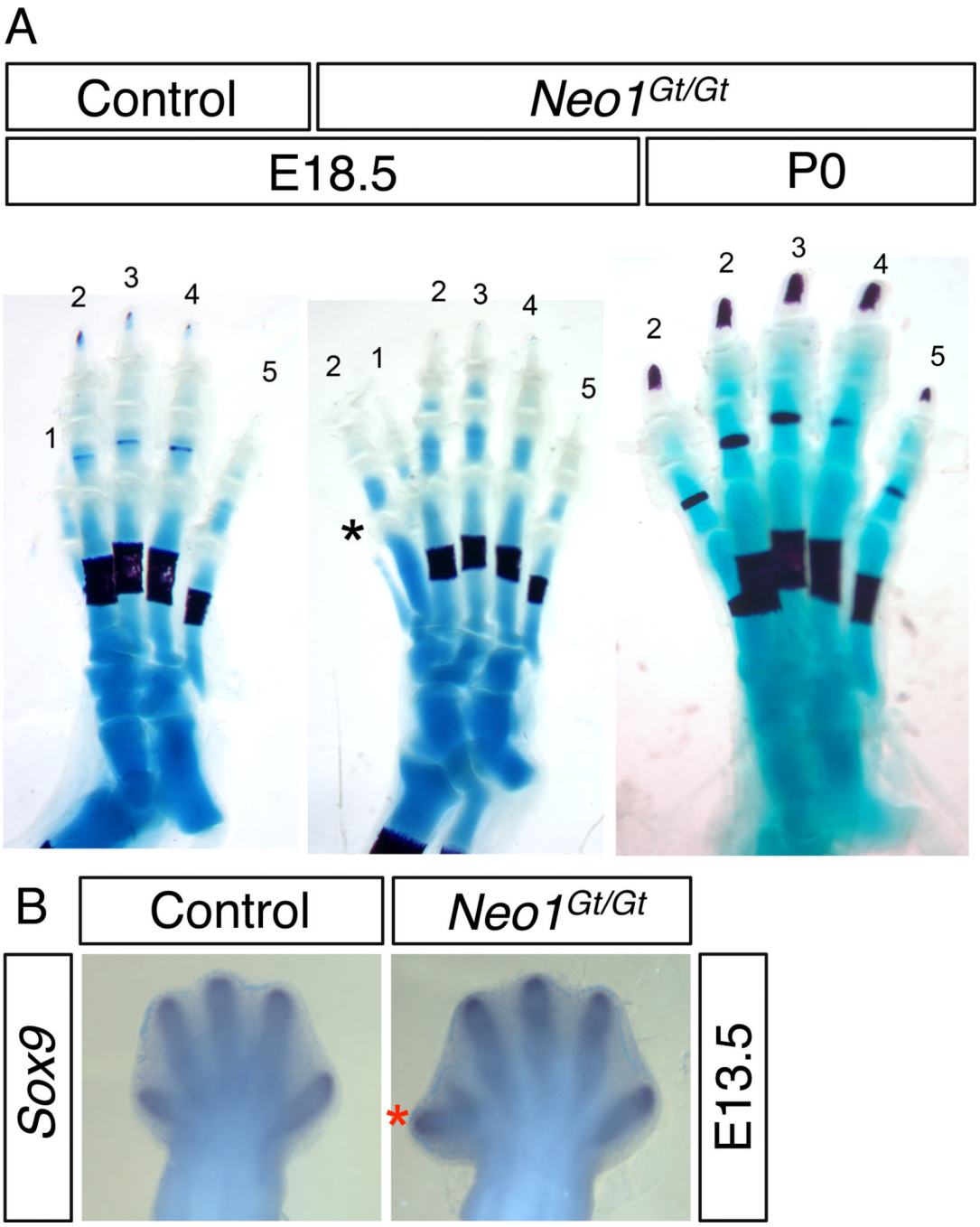

Fig. 1.

Neo1$^{Gt/Gt}$ mice display preaxial polydactyly. **A:** The right hindlimbs from control (*Neo1*$^{+/+}$ or *Neo1*$^{+/Gt}$) and *Neo1*$^{Gt/Gt}$ mice at E17.5 or P0, as indicated. Embryos were stained with Alizarin Red and Alcian Blue to identify bone and cartilage structures. Numbers over toes represent digit identity. Note that the *Neo1*$^{Gt/Gt}$ limb at E18.5 has an extra digit 2 and additional rudimentary metatarsal (asterisk) on the anterior side, whereas the *Neo1*$^{Gt/Gt}$ limb at P0 has an identity shift of digit 1 to digit 2. **B:** Whole mount in situ hybridization of the early chondrogenesis marker *Sox9* at E13.5. The red asterisk indicates an extra digit.

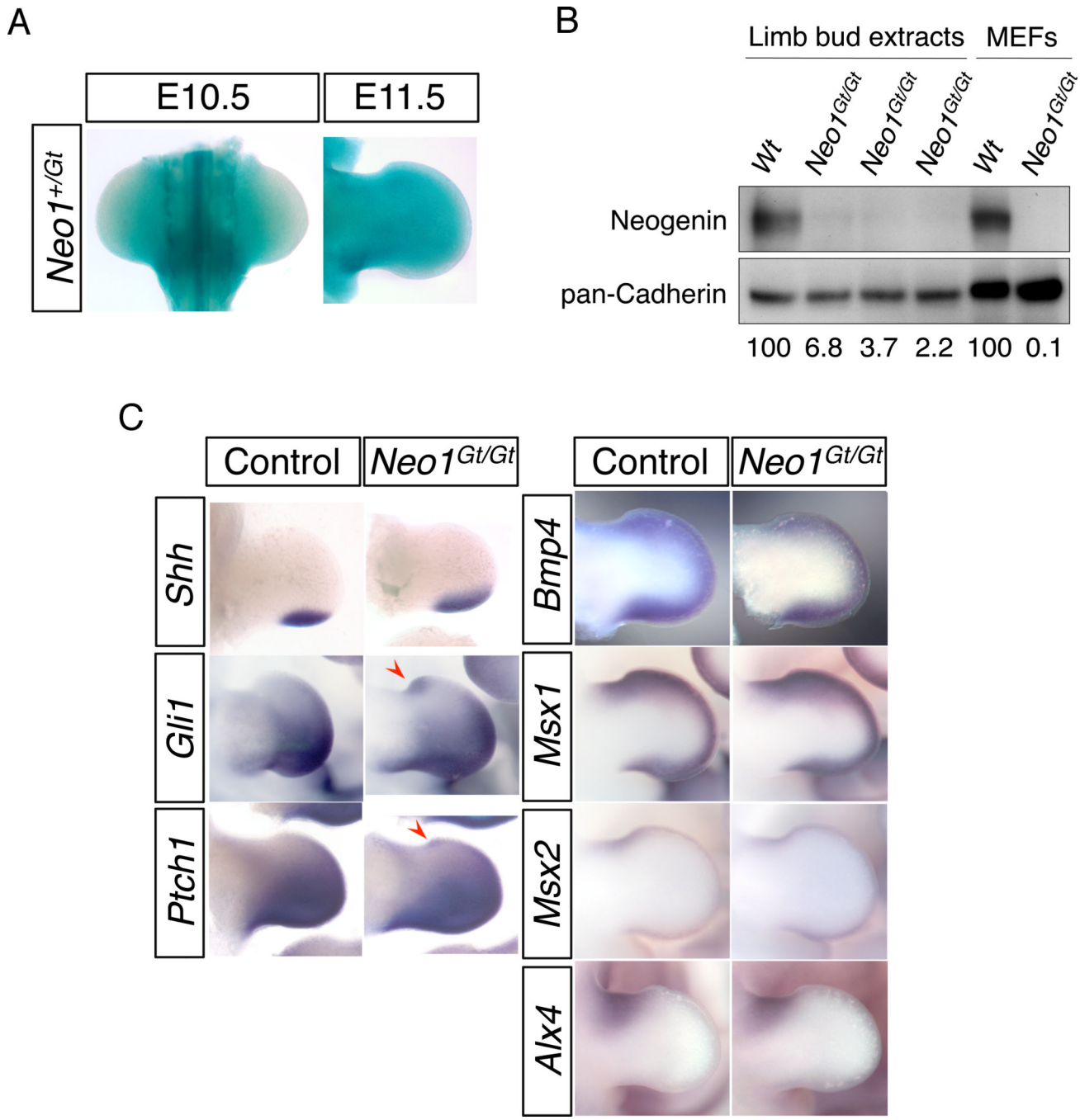

Fig. 2.

Expression of *Neo1* and limb patterning genes in control and *Neo1*$^{Gt/Gt}$ mice. **A:** Expression of the *Neo1-lacZ* reporter in E10.5 and E11.5 hindlimb buds. **B:** Western blot analysis of neogenin expression in E11.5 wild-type and *Neo1*$^{Gt/Gt}$ limb buds and in mouse embryo fibroblasts (MEFs). Blots were probed with neogenin and, as a loading control, pan-cadherin antibodies. Numbers below lanes represent the relative amounts of neogenin produced by limb buds of the indicated genotype, normalized to cadherin expression. A similar analysis was performed with MEFs, which were normalized independently from limb buds. **C:** Whole mount in situ hybridization of *Shh* (n=8), *Gli1* (n=8), *Ptch1* (n=10), *Bmp4* (n=10),

Msx1 (n=12), *Msx2* (n=12) and *Alx4* (n=10) expression in control (*Neo1*$^{+/+}$ or *Neo1*$^{+/Gt}$) and *Neo1*$^{Gt/Gt}$ right hindlimb buds at E11.5. Red arrowheads indicate ectopic anterior expression of *Gli1* and *Ptch1*.

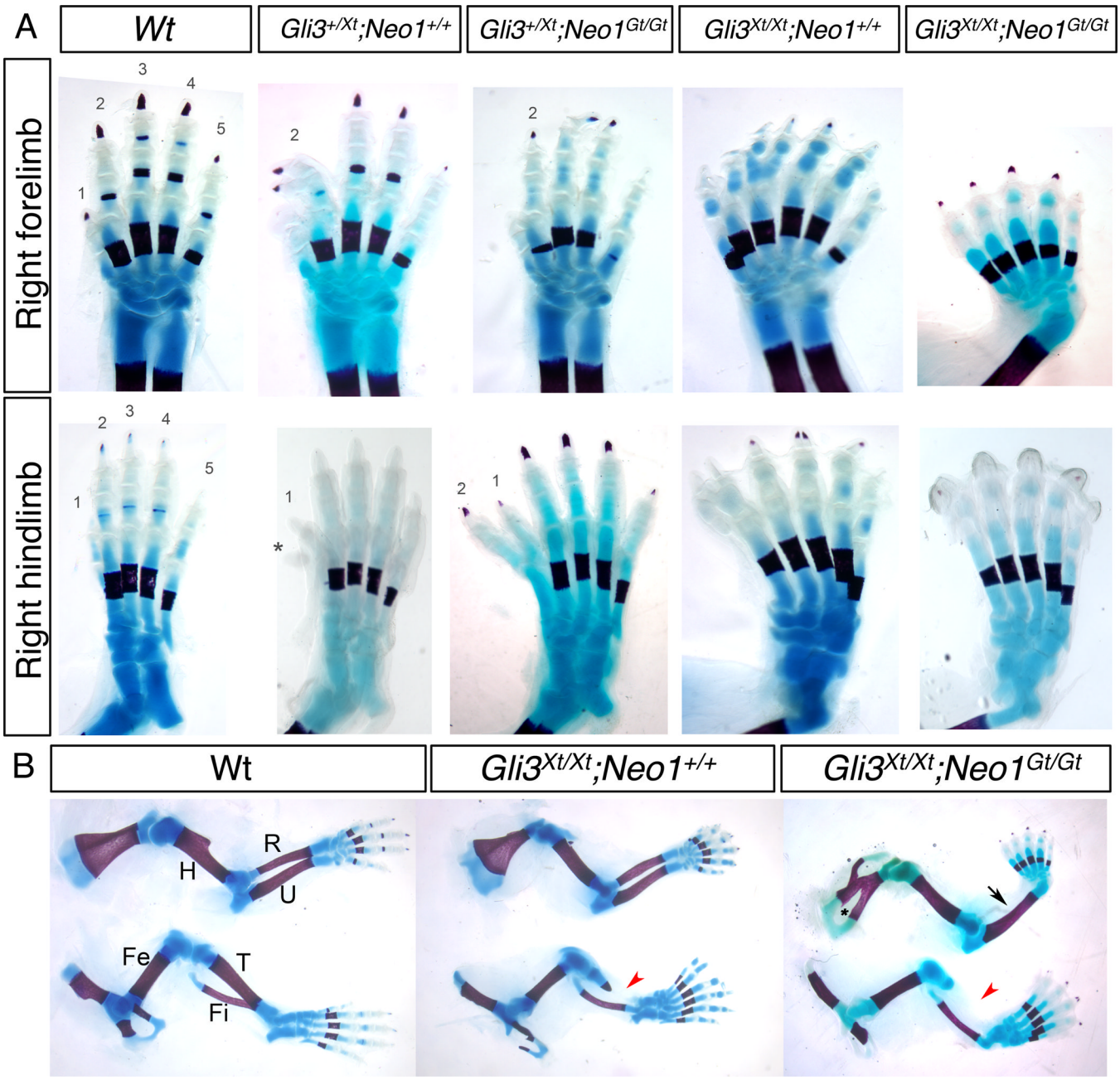

Fig. 3.

Autopod and zeugopod phenotypes of *Gli3;Neo1* double mutants. **A:** Bone and cartilage staining of autopods of E18.5 mice of the indicated genotypes. Numbers on digits represent their identity. The asterisk indicates a nubbin. **B:** Bone and cartilage staining of limbs of E18.5 embryos of the indicated genotypes. The upper and the lower rows represent forelimbs and hindlimbs, respectively. Note the absence of a radius in the $Gli3^{Xt/Xt};Neo1^{Gt/Gt}$ embryo (black arrow) and the rudimentary and absent tibias in the $Gli3^{Xt/Xt};Neo1^{+/+}$ and $Gli3^{Xt/Xt};Neo1^{Gt/Gt}$ embryos, respectively (red arrowheads). The asterisk represents reduced bone formation in the anterior stylopod of the $Gli3^{Xt/Xt};Neo1^{Gt/Gt}$ embryo. *Wt*, wild-type; H, humerus; R, radius; U, ulna; Fe, femur; T, tibia; Fi, fibula.

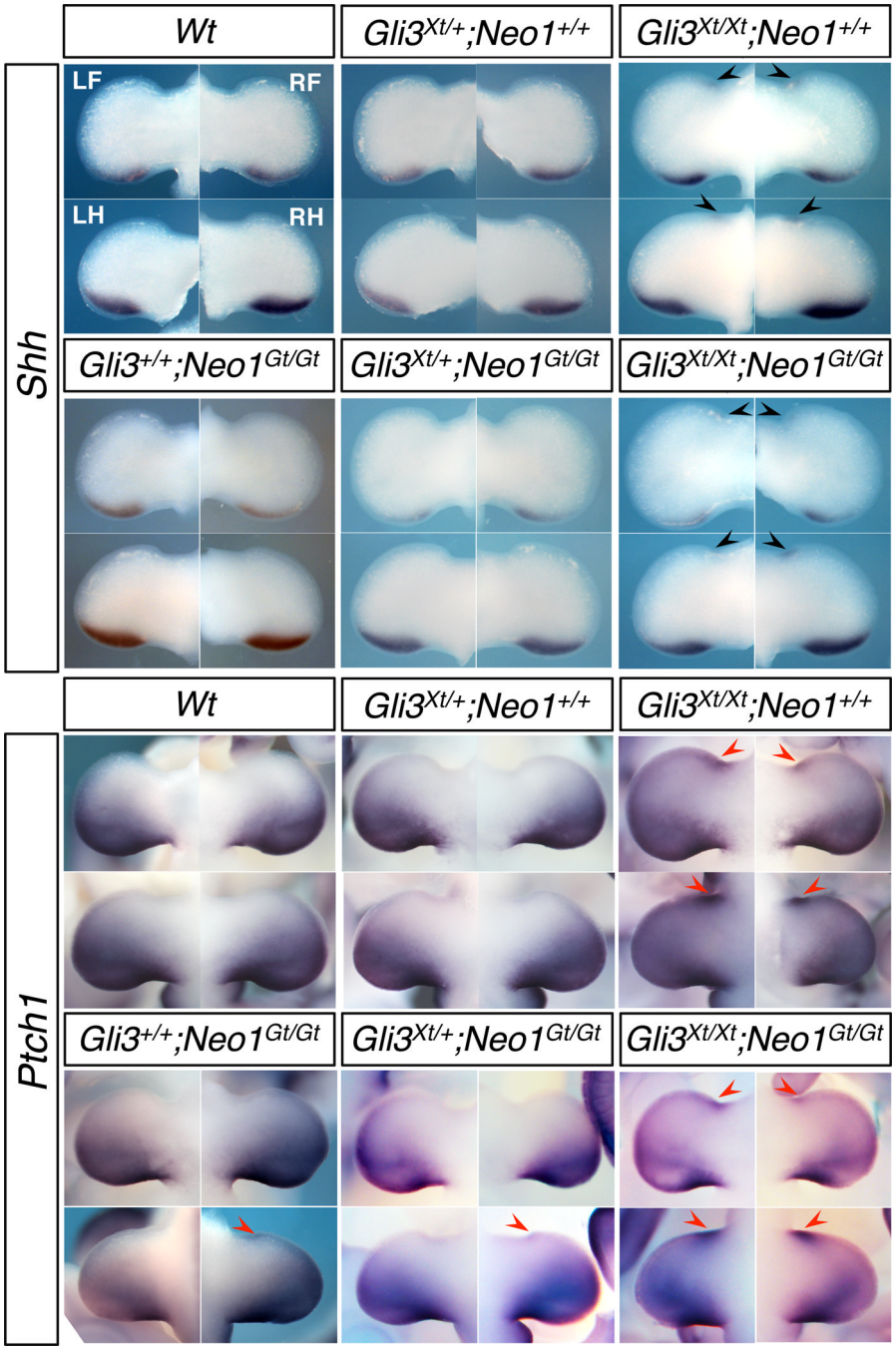

Fig. 4.

Expression of *Shh* and *Ptch1* in *Gli3;Neo1* double mutants. Whole mount in situ hybridization analysis *Shh* and *Ptch1* expression in E11.5 embryos of the indicated genotypes. Black arrowheads indicate ectopic anterior expression of *Shh*, red arrowheads indicate ectopic anterior expression of *Ptch1*. *Wt*, wild-type. LF, left forelimb; RF, right forelimb; LH, left hindlimb; RH, right hindlimb; all sets of limb buds correspond to the positions identified for the *Wt* set in the upper left of the figure.

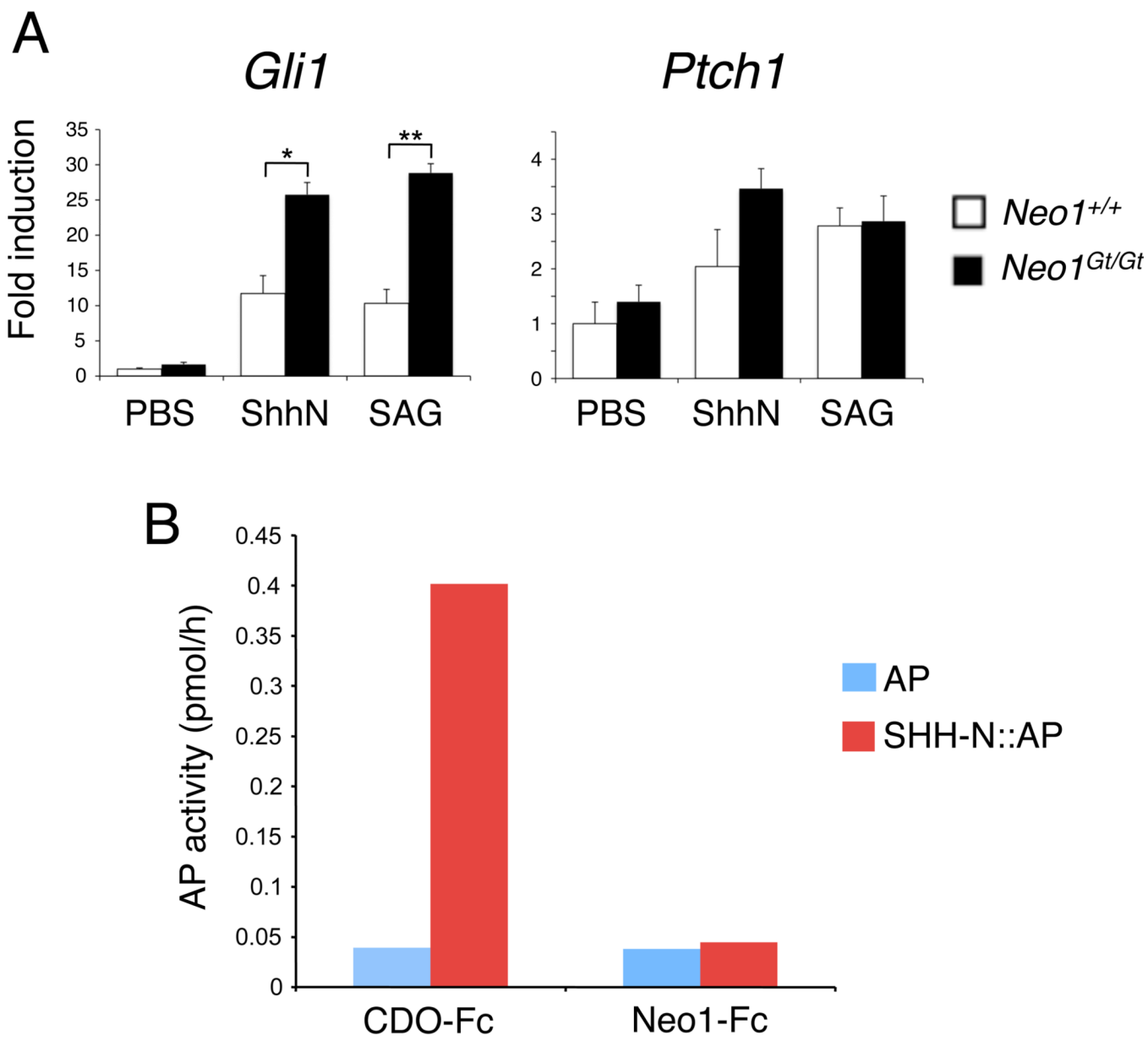

Fig. 5.

Neo1$^{Gt/Gt}$ MEFs are sensitized to SHH- and SAG-mediated *Gli1* induction but neogenin does not bind SHH. **A:** qRT- PCR analysis of *Gli1* and *Ptch1* expression in *Neo1*$^{+/+}$ and *Neo1*$^{Gt/Gt}$ MEFs. Two independent isolates of *Neo1*$^{+/+}$ MEFs and three independent isolates of *Neo1*$^{Gt/Gt}$ MEFs were analyzed in duplicate in three separate experiments. Data were normalized to expression of *Gapdh* presented as fold induction over control, PBS-treated WT MEFs. Data represent means ± S.E.M. and were analyzed by Student's t-test. *, $p < 0.02$; **, $p < 0.005$. **B:** Recombinant, secreted proteins comprising the ectodomains of neogenin or the SHH co-receptor, CDO, fused in-frame with the Fc region of human IgG (Neo1-Fc and CDO-Fc, respectively) were bound to protein-A sepharose. SHH-N::AP or, as a control, AP itself, were allowed to bind the Neo1-Fc and CDO-Fc matrices, which were then washed exhaustively. Bound AP activity was quantified with AP yellow liquid substrate.

Table 1

Extra-digit phenotypes of *Gli3*$^{+/Xt}$;*Neo1*^{Gt} double mutants.

	Limbs with extra digits[1] (%)			
Genotype	**Left hindlimb**	**Right hindlimb**	**Left forelimb**	**Right forelimb**
Gli3$^{+/+}$;*Neo1*$^{+/+}$ (n=3)	0	0	0	0
Gli3$^{+/+}$;*Neo1*$^{+/Gt}$ (n≥8)	0	0	0	0
Gli3$^{+/+}$;*Neo1*$^{Gt/Gt}$ (n≥14)	0	14.3	0	0
Gli3$^{+/Xt\text{-}J}$;*Neo1*$^{+/+}$ (n≥18)	5.6	16.7	40.9	78.9
Gli3$^{+/Xt\text{-}J}$;*Neo1*$^{+/Gt}$ (n≥11)	7.7	9.1	53.8	66.7
Gli3$^{+/Xt\text{-}J}$;*Neo1*$^{Gt/Gt}$ (n≥22)	27.3*	59.1*	0**	4.3**

[1]Numbers of digits were counted after bone and cartilage staining of E18.5 embryos.

*Different from *Gli3*$^{+/Xt\text{-}J}$;*Neo1*$^{+/+}$, p<0.01;

**different from *Gli3*$^{+/Xt\text{-}J}$;*Neo1*$^{+/+}$, p<0.0001.

Table 2

Suppression of polydactyly in *Gli3*$^{Xt\text{-}J/Xt\text{-}J}$;*Neo1*$^{Gt/Gt}$ mice.

Genotypes	Average numbers of digits/limb[1]	Animals with five digits on at least one limb (%)	Limbs with five digits (%)	Limbs with ≥7 digits (%)
Gli3$^{Xt\text{-}J/Xt\text{-}J}$;*Neo1*$^{+/+}$ (n=7)	6.6±0.3	0	0	50
Gli3$^{Xt\text{-}J/Xt\text{-}J}$;*Neo1*$^{+/Gt}$ (n=11)	6.3±0.2	0	0	21.4
Gli3$^{Xt\text{-}J/Xt\text{-}J}$;*Neo1*$^{Gt/Gt}$ (n=8)	5.7±0.5*	75	43.8	12.5

[1] Numbers of digits were counted after bone and cartilage staining of E18.5 embryos.

* Different from *Gli3*$^{Xt\text{-}J/Xt\text{-}J}$;*Neo1*$^{+/+}$, $p<0.0001$.